Journal of Polymer Research (2021) 28:431
https://doi.org/10.1007/s10965-021-02809-2

REVIEW PAPER

Physical aging of multilayer polymer films—influence of layer thickness on enthalpy relaxation process, effect of confinement

Khadidja Arabeche[1] · **Laurent Delbreilh**[2] · **Eric Baer**[3]

Received: 15 February 2021 / Accepted: 21 October 2021 / Published online: 24 October 2021

Abstract

The phenomenon of physical aging of glassy polymers in confined environments has been extensively studied over the last few decades due to its numerous technological and fundamental implications. Understanding aging in confined environments is vital for predicting the long-term performances in applicative conditions for confined glassy polymers. The physical aging of PC/PMMA multilayer films, with layer thicknesses ranging from micro-to-nanoscale, was explored using the Differential Scanning Calorimetry (DSC) technique. Reducing the layer thickness down to 12 nm was shown to have a very different effect on the structural relaxation parameters of the above-mentioned polymers. Recovered enthalpy data for aged films exhibited an acceleration in physical aging under confinement for PC (rigid backbone and rubbery environments), while no change was noted for PMMA (flexible backbone and amorphous environments). A large effect in the amplitude of the structural relaxation process has also been evidenced for confined PC layers. These observations have thoroughly been discussed with respect to the impact of the chemical structure (entanglement), adjacent polymer state (rubbery and amorphous environments) and the nature of molecular mobility (the CRR shape and length are both related to intra-chain and inter-chain relaxation during glass transition),. Moreover, it was found that the accelerated aging of PC was mainly attributed to the dynamic relaxation related to its chemical structure and local modification of intermolecular interactions.

Keywords Physical aging · Multilayer films · Confinement · Cooperativity · Glass transition

Introduction

A thermodynamic system brought out of equilibrium spontaneously evolves to go back to its equilibrium state. It is worth noting that the vitreous state is an out-of-equilibrium state of glass-forming liquids, and like any other non-equilibrium physical system, it will tend to return to the equilibrium state over time. The relaxation of thermodynamic properties in the vitreous domain, such as the volume or enthalpy with annealing time, is a phenomenon referred to as structural recovery.

During the structural relaxation process, molecules tend to rearrange for the purpose of minimizing the energy of the system. The structural relaxation phenomenon is generally associated with slow molecular motions within the material. This structural relaxation phenomenon (structural recovery), also called physical aging, engenders some changes in the physical, thermal, mechanical, electrical and optical properties of vitreous polymers. Unlike the chemical aging (oxidation, UV radiation, etc.) for which the changes are mostly irreversible, the physical aging [1, 2] is a totally reversible process through heat treatment.

In nanotechnology, the use of glasses confined to the nanometer length-scale is mandatory, but this can be problematic as some material properties are size-dependent [3]. It is widely admitted that reducing the size of a glass-forming liquid, from the micrometric to the nanometric scale (nanoconfinement), is accompanied by significant modifications of its properties, compared to the bulk [4–9].

✉ Khadidja Arabeche
arabeche.khadidja@yahoo.com

✉ Laurent Delbreilh
laurent.delbreilh@univ-rouen.fr

[1] Macromolecule Research Laboratory (MRL), Faculty of Sciences at Abou, Bakr Belkaïd University, Tlemcen, Algeria

[2] Normandie Univ, UNIROUEN, INSA Rouen, CNRS, GPM, 76000 Rouen, France

[3] Department of Macromolecular Science, Case Western Reserve University, Cleveland, Ohio 44106-7202, US

Furthermore, the new properties of nanoscale phases, in addition to their technological interest, are often associated with fundamental research questions that are totally open to the field of condensed matter physics [8, 10–13].

Quite a number of research teams have studied the glass transition of polymers in a confined environment using different techniques [14–19]. The variations in the temperature Tg were observed for the first time in layers of thicknesses in the order of 100 nm; this phenomenon is emphasized for thicknesses ≤ 40 nm [20]. The experimental results [21–24] obtained for nanoscale films, numerical simulations [25–29] and theoretical approaches [30–32] allowed to evidence some changes in the glass transition temperature Tg as well as in the structural relaxation (physical aging) [33–36]. The variations in Tg and in the aging rates could be either greater or smaller than the value measured in bulk material.

Therefore, in order to be able to predict the long-term performance of polymers, it is necessary to understand their aging process under nanoscale confinement. Recently, a number of studies on the physical aging of glassy polymers have indicated that the aging behavior is often highly affected by its confinement environment; among these are polymer thin films, nanocomposites [37], nanoporous polymers [38] and nanotubes [39]. In addition, some studies reported that aging could be reduced or completely prevented, while others found out that the physical aging was more accelerated in a nanostructured materiel than in the bulk. This may be explained by the interfacial interactions:

- A free surface (interface) where little interaction of the film with the substrate occurs induces an increase in the molecular mobility near that surface, which leads to an acceleration of physical aging. This is generally attributed to the decrease in Tg [40–42] in a confined environment (driven force).
- Strong interactions with the substrate immobilize the polymer chains in the vicinity of the interface, reduce the molecular mobility and disrupt glassy dynamics. This causes an increase in the Tg value [40, 43] and prevents or slows down the physical aging in a confined environment [44].

However, the interfacial effects do not explain all the anomalies of molecular dynamics and the contradictory results from studies on glass transition and physical aging in confinement geometries. For example, the enhanced physical aging under confinement for unsupported films [45] and the reduction in physical aging rate at the air-polymer interface of PMMA films [46] cannot be explained only by the interfacial effects.

In this context, Priestley, Campbell et al. [47, 48] indicated that the size and flexibility of monomer units play a significant role; they also suggested that the associated side groups seem to influence the behavior of glass transition temperature (Tg).

These findings suggest that the dynamics of the cooperative segments play an essential role in the behavior of Tg. Indeed, several studies have reported some variations in the molecular dynamics of confined films when assessing the relaxation time by using the Dielectric Relaxation Spectroscopy (DRS) [49, 50], or by calculating the characteristic length of Cooperative Rearranging Region (CRR) ξ through the use of Temperature modulated differential scanning calorimetry (TMDSC) [51, 52].

The difference in length-scale, for which confinement can affect the physical aging of various polymers, is greater than 1 micron for polysulfone and PC (rigid backbones) [45, 53] and less than 300 nm for PMMA and PS (flexible backbone). It was found that the chemical structure appears to play a significant role in the way confinement impacts physical aging. The different confinement's conditions such as hard versus soft confinement can also impacts the processes of aging.

Furthermore, it is generally acknowledged that the impact of confinement on aging depends on the conditions under which the process takes place, such as the stress induced during film quenching [54], the memory effect, aging temperature and the type of confinement…etc.

More particularly, the study of the physical aging process in multilayer polymers seems to be of the utmost importance, not only because their long-term material performances are essential to their optimal use in various applications, but also because few studies have characterized the structural relaxation of multilayer confined polymers, and only even fewer have investigated the effect of the confined environment on the physical aging process. It is worth noting that this effect is associated with the nanostructured aspect of the multilayer polymer [55, 56], the molecular structure, the state of each polymer during aging, and the nature of molecular movements within the range of glass transition.

In order to investigate the influence of nanoconfinement on the physical aging process, layer-multiplying coextruded films of polycarbonate (PC) and poly (methyl methacrylate) (PMMA) films, containing tens to thousands of layers with individual layer thicknesses from the microscale to the nanoscale, are examined in the present study.

To do this, it was decided to examine the complex structure of our samples and analyze the effect of confinement and the different mechanisms occurring at the interface between the layers.

Experimental

Materials and processing

The materials used in this work are multilayer films comprising alternating layers of bisphenol-A polycarbonate (PC) and atactic poly (methyl methacrylate) (PMMA) which are both amorphous polymers. Polycarbonate (Caliber 200 -10), which was provided

by Dow Chemical Company, has an average molecular weight (M_w) of 62 kg.mol^{-1}; its volumetric mass (ρ_{PC}) is 1.1934 g.cm^{-3}, and the molar mass of one monomer unit is M_0 = 254 g.mol^{-1}. With regard to Polymethyl-methacrylate (Plexiglas V826), it was provided by ATOFINA Chemicals Inc.; its average molecular weight (M_w) is 132 kg.mol^{-1}. The volumetric mass of PMMA (ρ_{PMMA}) is 1.1923 g.cm^{-3} and the molar mass of one monomer unit M_0 is 100 g.mol^{-1}.

The multilayer films, having different thicknesses, were produced by the multilayer co-extrusion technique at the Department of Macromolecular Science and Engineering, Case Western Reserve University (CWRU) in Cleveland, Ohio (USA). This technique allows for the fabrication of multilayer films comprising two or more polymers alternated with thousands of layers. The nomenclature adopted for the sample was PC/PMMA-*X*, where *X* is the number of layers as indicated in Table 1.

In the present work, the multilayer films, PC/PMMA-08, PC/PMMA-32, PC/PMMA-1024 and PC/PMMA-4096, were examined. Each film has a PMMA/PC composition ratio of 50:50 by volume.

Differential Scanning Calorimetry (DSC)

The isothermal physical aging of PC/PMMA multilayer films was investigated at two different temperatures by means of a TA Instruments Q100 Differential Scanning Calorimeter (DSC). This apparatus was calibrated for the measurement of heat flow, temperature and baseline (sensor capacitance for T_{zero} technology) using the standard calibration procedure (melting enthalpy and temperature of Indium and melting temperature of Zinc). Measurements and heating ramp have been carried out with heating and cooling rates $\beta_h = |\beta_c| = 10$ K/min. The selected aging temperatures were chosen below the Tg of PMMA for the first study of structural relaxation of PMMA at $T_a = 100$ °C; a second aging temperature was chosen below the Tg of PC and higher than PMMA Tg, in order to study the structural relaxation of PC at $T_a = 100$ °C. The same thermal history and aging times (t_a) were applied to all multilayer films.

Table 1 Sample codes, number of layers, and individual layer thicknesses of the samples

Sample code	Number of layers	Individual layer thickness
PC/PMMA-08	**8**	**16 µm**
PC/PMMA-32	**32**	**4 µm**
PC/PMMA-1024	**1024**	**125 nm**
PC/PMMA-4096	**4096**	**12 nm**

Results and discussion

Structure of extruded PC / PMMA layers and PC / PMMA layers subjected to thermal cycles

Figure 1 depicts two AFM tapping mode phase images for the same multilayer PC/PMMA-4096 film, after the temperature ramp of 180 °C (left), and after a measurement cycle where the PC/PMMA-4096 multilayer film was heated at the rate of 10 °C/min to 180 °C, and was then was subjected to thermal annealing from 0 to 6000 min (right) (from Arabeche et al. [57]).

Furthermore, it turned out that, before and after annealing, the multilayer films composed with PC and PMMA revealed an alternating layered architecture that was continuous and almost uniform throughout the film sample, on the macroscale and nanoscale. It can therefore be concluded that the annealing treatment did not have an impact on the multilayer structure. These findings are very different from those found, for example, by Bernal-Lara et al. [58] who investigated the nanolayers of polyethylene films and found out that they were not stable when the temperature exceeded the melting point of PE.

Aging of PMMA layers below the glass transition temperature

The effect of film thickness on the physical aging of poly (methyl methacrylate) (PMMA) layers supported on PC layers was examined by means of the Differential Scanning Calorimetry (DSC) technique. Multilayer films were aged at the temperature $Ta_{PMMA} = 100$ °C with aging times t_a: [30 min: 6000 min].

Figure 2 presents the DSC thermograms obtained during the heating ramp just after the isothermal physical aging step for all the aging times (t_a) for PC/PMMA-08, PC/PMMA-1024, PC/PMMA-4096. The physical aging evolution of PMMA was confirmed by the appearance and the evolution with aging time of an enthalpy peak superimposed to the heat capacity endothermic step of PMMA at Tg. This enthalpy relaxation is observed for all multilayer samples, as shown in Fig. 2.

It should be noted that for long aging times, a slight evolution of the endothermic peak superimposed to heat capacity step at the glass transition of the polycarbonate, was observed. This observation suggests that vitreous PC undergoes the physical aging phenomenon with a very slow kinetics even if the isothermal relaxation protocol is carried out 45 K below the Tg of PC.

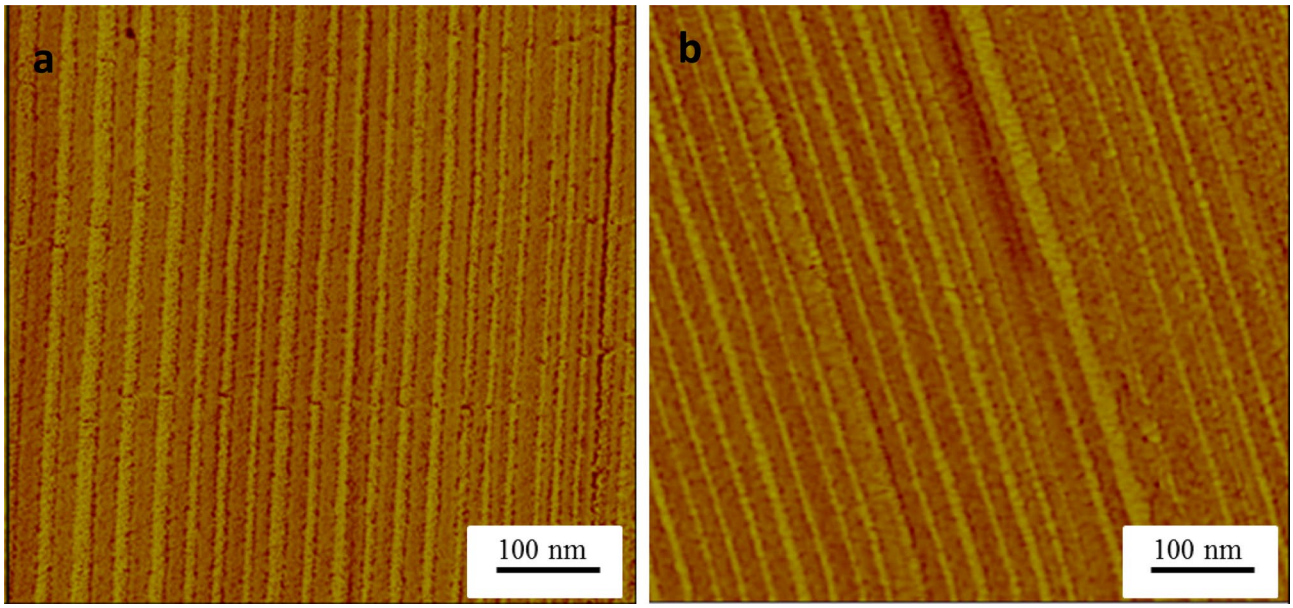

Fig. 1 AFM taping Images of 50/50 PC/PMMA multilayer films obtained for (PC/PMMA-4096). (**a**) After a temperature ramp to 180 °C. (**b**) Film after thermal cycles for various aging times from 60 °C to 180 °C. (from Arabeche et al. [57])

Aging of PC layers below the glass transition temperature

The effect of film thickness on the physical aging of polycarbonate (PC) layers, supported on PMMA layers, was determined by means of the differential scanning calorimetry (DSC) technique. The multilayer films were aged at $Ta_{PC} = 130$ °C with t_a: [30 min: 6000 min].

An increase in the heat flow overshoot with increasing aging time was observed in all multilayer composite samples in the glass transition domains of PC, as it is clearly illustrated in Fig. 3. This effect is characteristic of relaxation effect for isothermal aging below Tg or it can be observed also due to differences between cooling and heating rates during vitrification/devitrification [59, 60]

Note that for the same aging time, an enthalpy reduction associated with an endothermic overshoot for confined films (PC/PMMA-4096 and PC/PMMA-1024) was observed, which is not the case for bulk films PC/PMMA-08 and PC/PMMA-32. One may clearly see that the endothermic peak of nanolayers is less pronounced and wider than that measured for bulk films. This observation suggested a reduction in the aging rate with confinement [55, 61].

The curves plotted in Figs. 2 and 3 can be used to determine the evolutions of the recovered enthalpy ΔH. The recovered enthalpy was estimated from the experimental DSC thermograms of aged samples (aging time t_a), and rejuvenated same sample ($t_a = 0$) according to Eq. (1) given below [62].

$$\Delta H = \int_{T1}^{T2} \left[Cp^{aged}(T) - Cp^{ref}(T) \right] dT \tag{1}$$

where T_1 is a temperature well below Tg and T_2 a temperature well above Tg in liquid equilibrium state.

To compare the recovered enthalpy values of the layered and bulk films, the values calculated must be normalized by the mass fraction (ω_{PMMA} and ω_{PC}) of each sample using Eq. (2) and (3).

$$\Delta H_{PMMA} = \frac{\Delta H_{layered,total}}{\omega_{PMMA}} \tag{2}$$

$$\Delta H_{PC} = \frac{\Delta H_{layered,total}}{\omega_{PC}} \tag{3}$$

ω_{PMMA} and $\omega_{PC} = 0.5$ for the samples presented in this work.

As can be clearly seen from Fig. 4, it is difficult to differentiate the evolutions of ΔH for PMMA glass transition as a function of aging time for the different layer thicknesses. Consequently, it can be stated that there is no apparent changes in the structural relaxation kinetics of PMMA as a function of the layer thickness of the layers.

Comparing the evolution with aging times of the values of enthalpy ΔH_{PMMA} allows stating that layer thickness has a very weak influence on the physical aging process of PMMA glass transition.

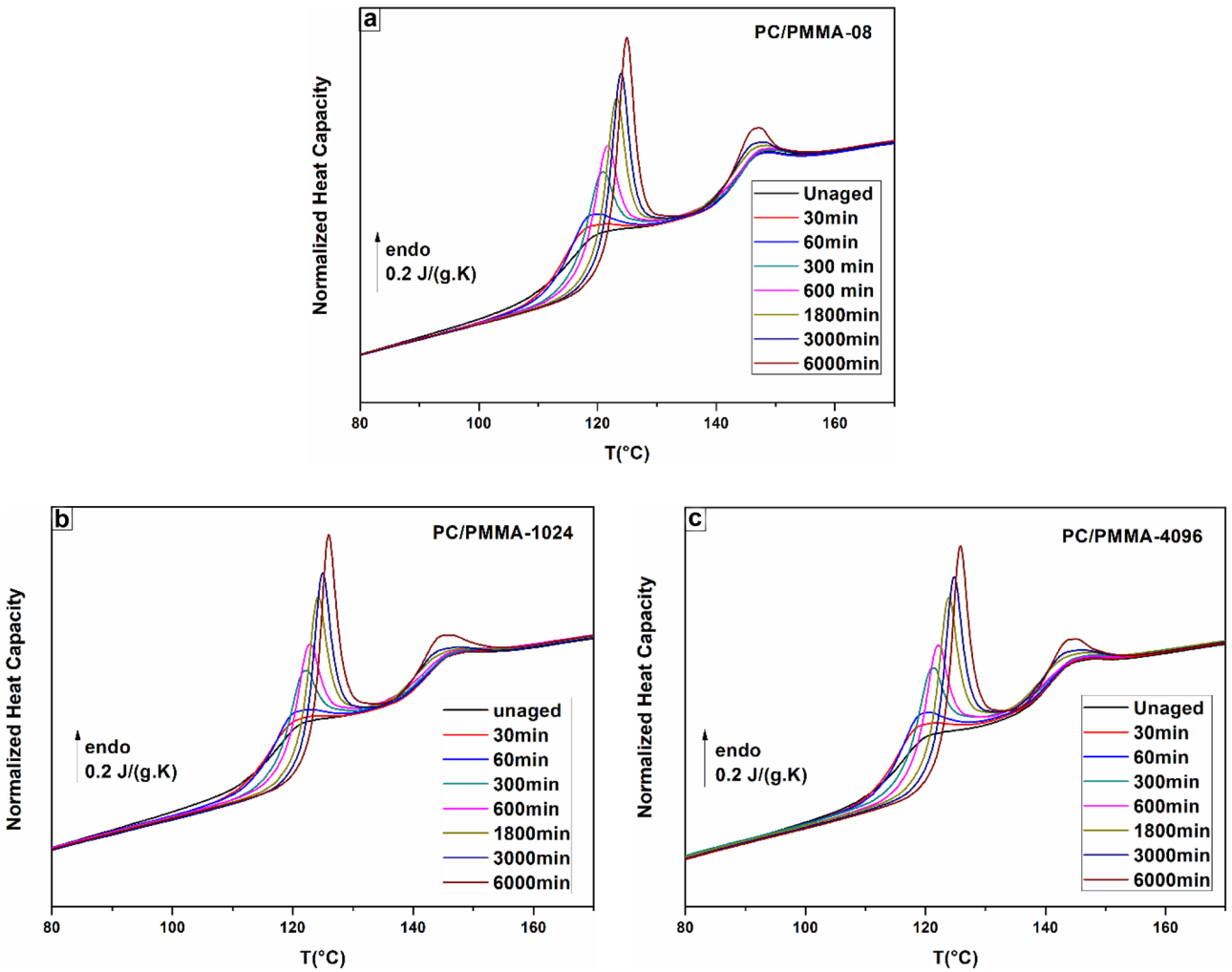

Fig. 2 DSC curves obtained for the multilayer films: **(a)** PC/PMMA-08, **(b)** PC/PMMA-1024, **(c)** PC/PMMA-4096, with a heating rate of 10 K min^{-1} after aging the samples at 100 °C; the aging times are as indicated on the thermograms

For PC recovered enthalpy vs. aging ta, a clear difference can be observed on Fig. 5, compared to what has been obtained for PMMA recovered enthalpy (Fig. 4).

The recovered enthalpy for PC/PMMA-08 and PC/PMMA-32, are quite similar to what is observed for PMMA Δh. PC/PMMA-1024 and PC/PMMA-4096 reach a plateau value of the recovered enthalpy when their thickness changed from microscale to nanoscale (the plateau is achieved in almost 100 min for layer thickness of 12 nm and 500 min for layer thickness of 125 nm). However, the plateau was not achieved at the macroscale, for PC but also for PMMA. This difference suggests that the enthalpy relaxation kinetic is quite impacted by the reduction of thickness of PC layers and occurs at a shorter time scale.

Enthalpy relaxation processes, present classically an ideal sigmoidal variation that can be numerically adjusted by a Kohlrausch–Williams–Watts function [63–66]:

$$\Delta H(t) = \Delta H_{\infty}.\left(1 - exp\left[-\left(\frac{t}{\tau}\right)^{\beta}\right]\right) \quad (4)$$

where $\beta < 1$ is the stretching exponent and τ is a characteristic relaxation time of the aging process.

ΔH_{∞} is the equilibrium enthalpy recovery theoretically obtained for an infinite aging time.

KWW stretched exponential decay functions are generally used in the literature to adjust numerically structural relaxation function obtained in glass-forming liquids in the vicinity of the glass transition temperature [67–69].

It can be calculated on a glass maintained at a temperature Ta < Tg, the expected total enthalpy recovery ΔH_{∞} extrapolated from the equilibrium liquid variation depends on the aging temperature T_a, as well as on the glass transition temperature Tg and the heat capacity step ΔCp of the sample, according to the following relation:

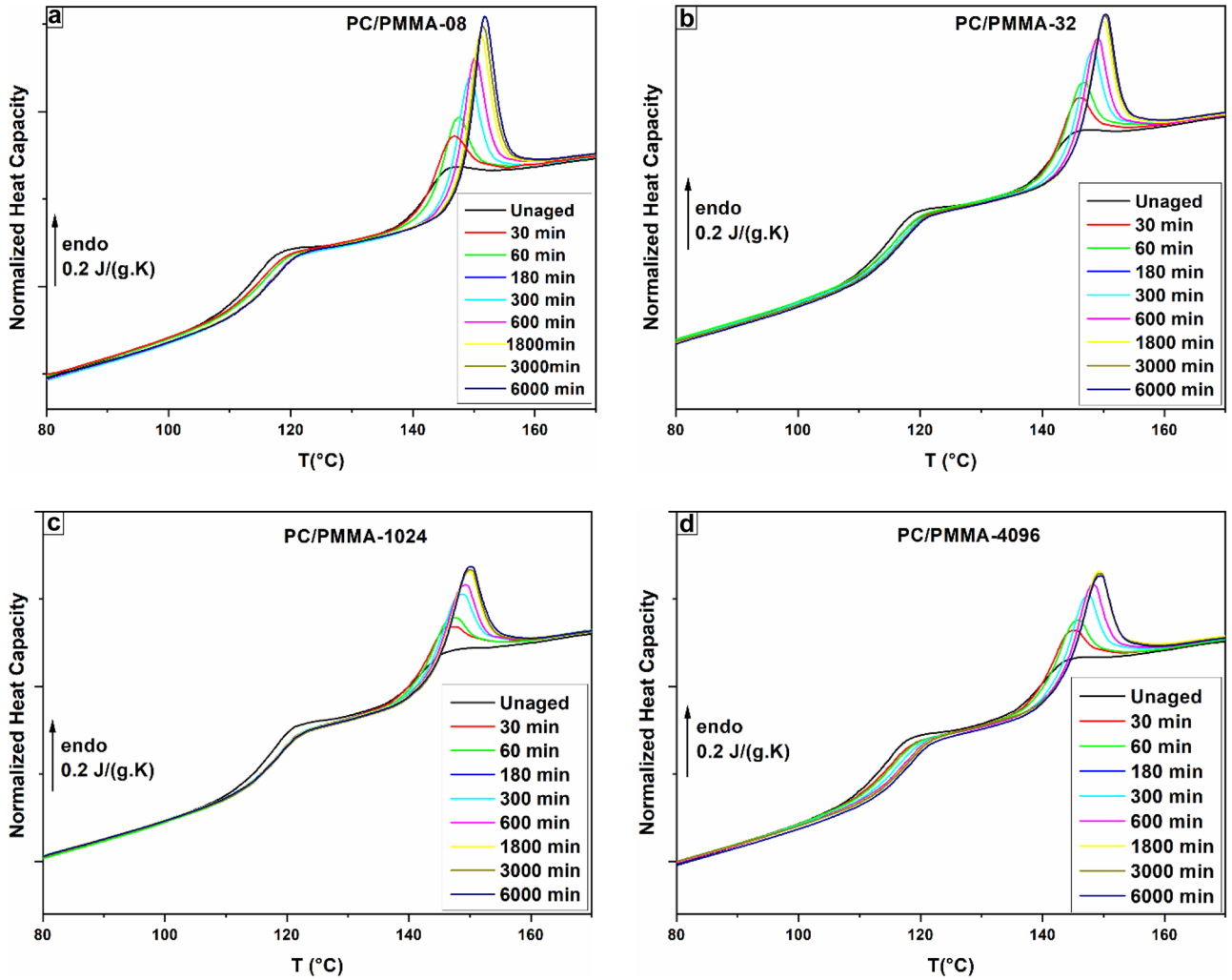

Fig. 3 DSC curves obtained for the multilayer films: (**a**) PC/PMMA-08, (**b**) PC/PMMA-32, (**c**) PC/PMMA-1024, and (**d**) PC/PMMA-4096, with a heating rate of 10 K min^{-1} after aging the samples at $T_a = 130$ °C; the aging times are indicated on the thermograms

$$\Delta H_\infty = \Delta C_p(T_g - T_a) \tag{5}$$

In literature, the nonexponential and nonlinear behavior of physical aging is established [70–73] and is often described by the Tool, Narayanaswamy, and Moynihan (TNM) model [74, 75]. The TNM model utilizes the Kohlrausch–Williams–Watts (KWW) [76] function to represent structural relaxation during aging and the enthalpy recovery phenomena can be described following the Eqs. (6):

$$\frac{\Delta H_\infty - \Delta H_t}{\Delta H_\infty} = exp\left[-\left(\frac{t}{\tau}\right)^\beta\right] \tag{6}$$

The normalized function Φ is used to show the evolution of the kinetic aspect of the aging for all PC sample. It enables a comparison of the entire enthalpy relaxation process with a normalization on the amplitude of this process (ΔH_∞):

$$\Phi(t_a) = \frac{\Delta H_\infty - \Delta H_{relaxation}(t_a)}{\Delta H_\infty} \tag{7}$$

The calculated relaxation functions are superimposed in Fig. 6 for PC the physical aging processes of all the multilayer samples. KWW fit relaxation functions (Eq. 6) have been used to compare the evolution of the relaxation time of the relaxation function as a function of PC layer thickness. ΔH_∞ experimental values and KWW parameters from fittings of experimental data presented in Figs. 4, 5 and 6 are reported in Table 2.

As it can be seen in Fig. 4 and Table 2 no clear evolution of the enthalpic relaxation process can be noted for PMMA

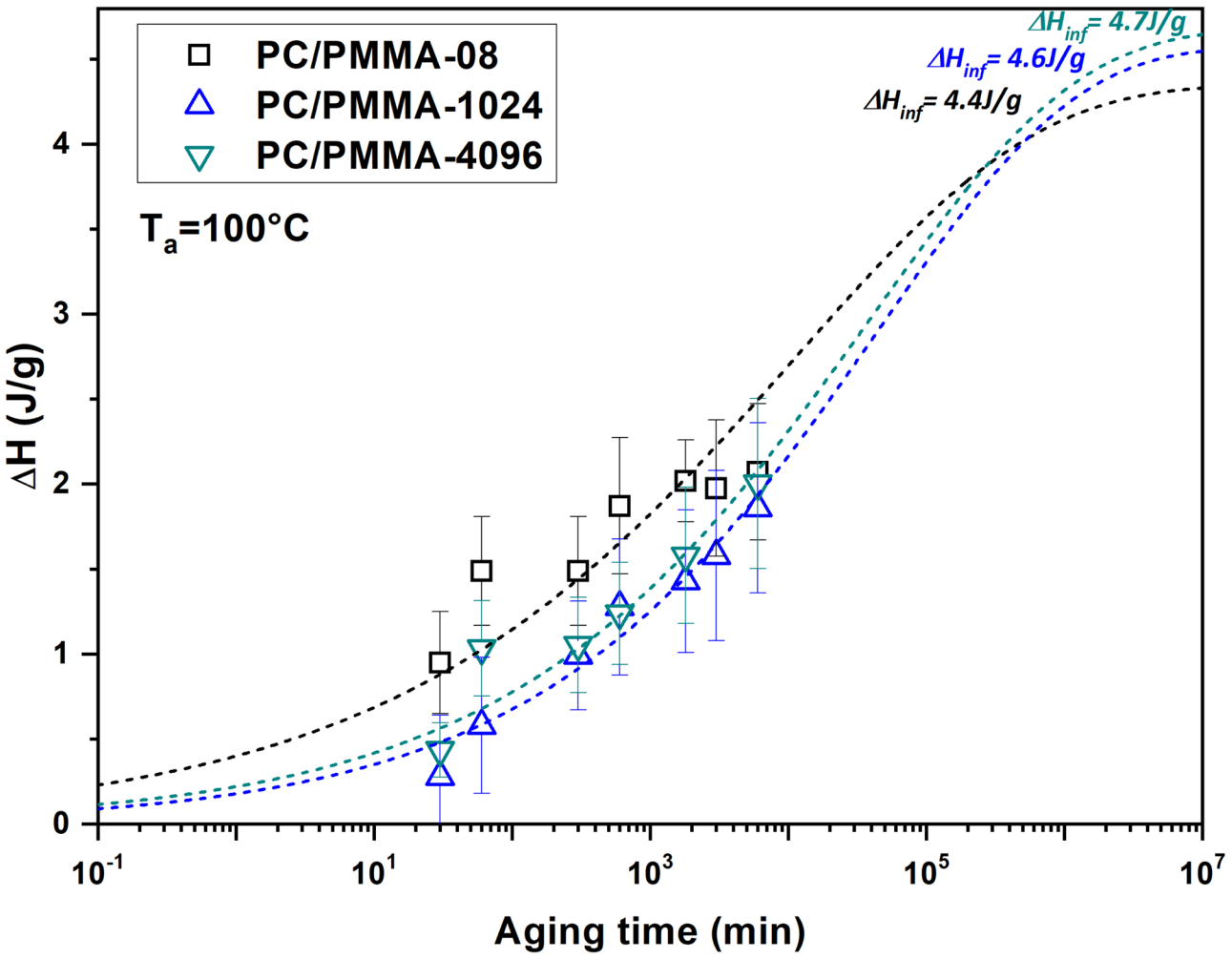

Fig. 4 Recovered enthalpy calculated as a function of aging time (t_a) for PMMA in multilayer films at $T_a = 100$ °C. The dotted lines are the results of KWW fitting model

glass transition with the evolution of the layer thickness. For PC glass transition two main evolutions can be discussed from the results presented in Figs. 4, 5 and Table 2.

First, it is clearly observed that the relaxation curves reach the equilibrium plateau in much shorter time for the PC in nanometer scale samples (125 nm and 12 nm), than samples with thicknesses in the micrometer range. The aging equilibrium plateau is actually reached in the aging time scale for the two thinnest samples. For PC with layer thickness in micrometer range the equilibrium enthalpy is not reached in the aging time scale of the experiments. This effect is attributed to a clear acceleration of the aging process in very thin samples in the range of nanometers, and this is confirmed by plotting the evolution of the relaxation time obtained by KWW fittings, as shown in Fig. 7: Even though the glass transition shift of 4 K may also accelerate the aging process due to a reduction of Tg-Ta value the huge amplitude of variation of τ vs. layer thickness (Fig. 7) is mainly attributed to the acceleration of molecular mobility due to several types of confinement effects [77–80].

Secondly as presented in Fig. 5 and Table 2, a remarkable difference is observed, for PC with layer thicknesses of 125 nm and 12 nm, between the equilibrium enthalpy recovery, ΔH_∞, reached experimentally and the calculated value from Eq. 4. This effect could be attributed to several molecular modifications associated to a confinement effect. For instance during accelerated aging processes measured using Fast Scanning Calorimetry some authors observed a variation of ΔH vs. t_a in two steps with an intermediate plateau [80, 81]. The plateau observed for the confined PC samples (Fig. 5) could be interpreted as an intermediate plateau without the possibility to see the second step regarding the aging time needed to observe this phenomenon as discussed earlier or as a reduction of the theoretical ΔH_∞ value du to a confinement effect on the molecular mobility of PC macromolecular chains.

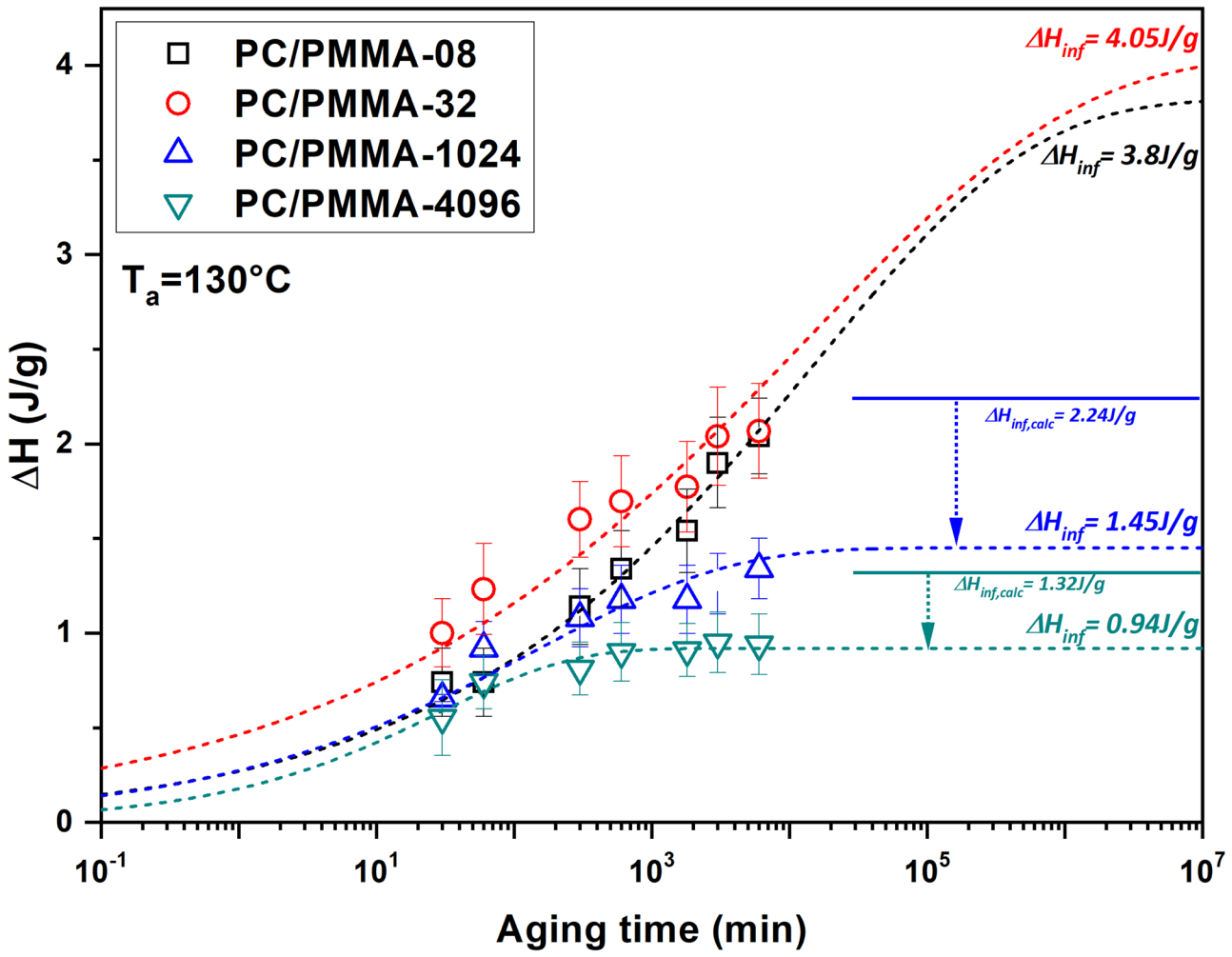

Fig. 5 Variations of recovered enthalpy as a function of the aging time for PC. The dotted lines are the results of KWW fitting model

Moreover, the acceleration of the physical aging process and the reduction of the theoretical ΔH_∞ value in PC nanolayered films is supported by our previous conclusions on the effect of confinement on Tg of multilayer films [57]. These results presented an increase in δT (peak width of Tg at half height) occurred for the nanolayered PC films, indeed, it rises from 3.36 °C for PC/PMMA-8 to 5.5 °C for PC/PMMA-4096. This increase was assigned to the large distribution of relaxation times and a decrease of Cooperative Rearranging Regions (CRR) size. The decrease in the size of CRRs with the confinement means that the molecular dynamics (mobility) of the chains become faster with confinement due to some reduction of intermolecular interactions between PC macromolecular chains.

The multilayer sample was held at an aging temperature of 130 °C so that the PC layers are in their glassy state (Tg of bulk PC = 150 °C), while the PMMA layers were in their rubbery state above Tg (Tg of bulk PMMA = 118 °C). This condition could be associated to a so-called "soft-confinement", while the effect of PMMA layers surrounded by vitreous PC could be considered as a "hard-confinement" [34]. Therefore, the polycarbonate chains were confined between the PMMA chains in the rubbery state, which suggests that the rubbery PMMA layer could have acted in a similar manner as a free surface (interface). In this regard, Amit and Robert [29] investigated the local dynamics of glass-forming polymers under nanoscale confinement, using molecular dynamics simulation. They found out that these dynamics on the surface of films were more than three times faster (lower τ) than inside the films, while the aging rate was more than two times larger in the middle than on the surface. They also reported that both the relaxation time and physical aging rate were lower on the surface, which fits well with our results.

On the other hand, Roth and collaborators indicated that both Tg and the physical aging rate of polymer thin films can be dramatically altered by adjacent polymer layers [82]. Similarly, Lewis and coworkers suggested that the aging rate

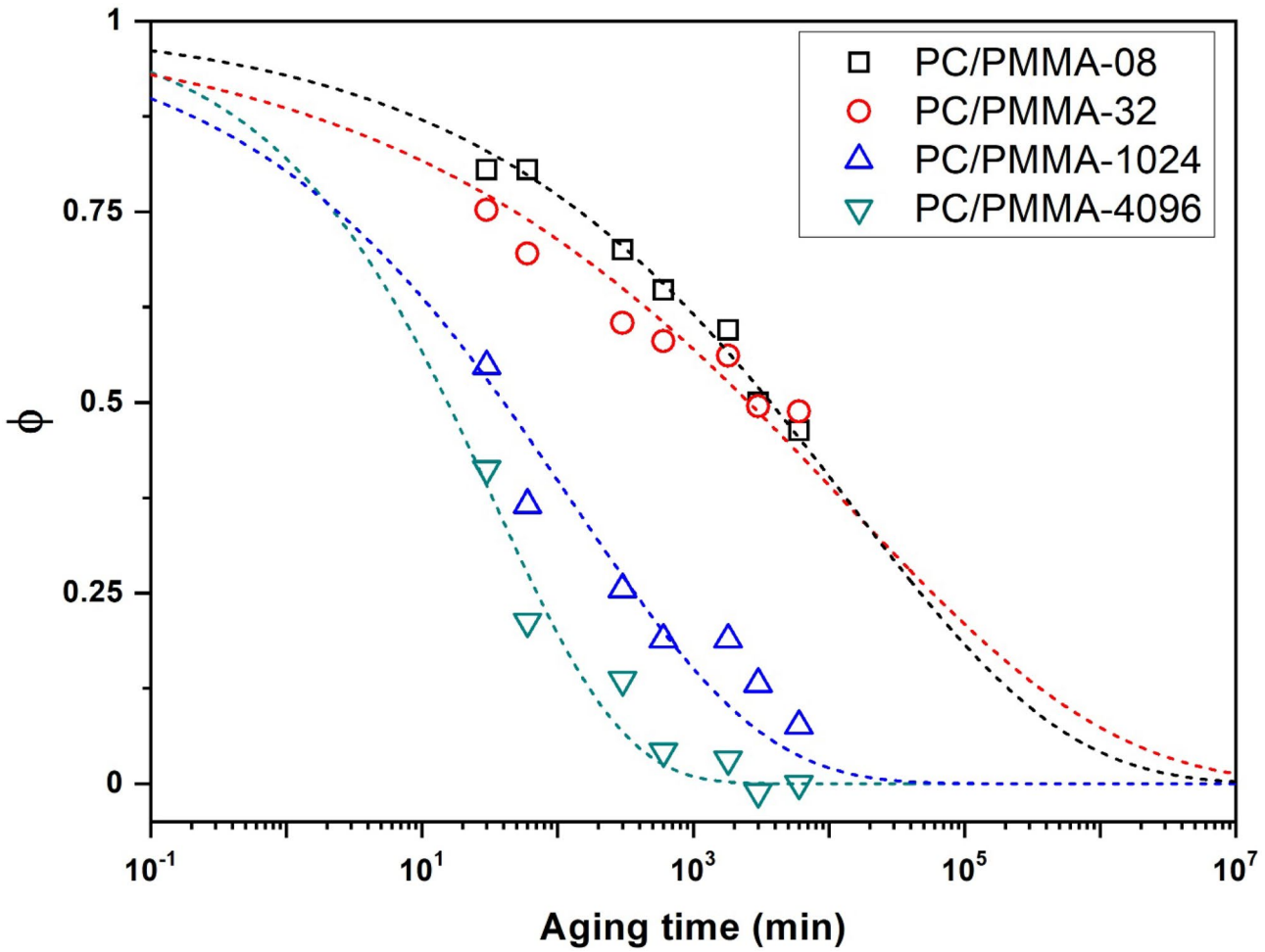

Fig. 6 Recovery function from enthalpy recovery versus aging time for PC films (Ta = 130 °C), dashed lines represents KWW fit relaxation functions (Eq. 6)

in polymer thin films decreases and the extent of this diminution depends on the adjacent layer [83].

The intensity of confinement of PC between PMMA rubbery layers becomes more important as the number of PMMA layers rises in multilayer films (larger contact between PC and PMMA), which leads to accelerated PC aging. This result suggests that the neighboring polymer (PMMA in this case) could strongly affect the dynamics of its adjacent layer in the multilayer film. The results obtained for the physical aging of polycarbonate (PC) softly confined between the PMMA layers in the multilayer PC / PMMA films are qualitatively consistent with those found in studies reported in the literature [55].

In the case of polycarbonate (PC), the confinement environment is soft (rubbery interface); therefore, it will not hinder the relaxation at the interface, which can facilitate the aging process. However, the PMMA chains were confined between hard walls (rigid amorphous polycarbonate

Table 2 ΔH_{∞} experimental values and KWW parameters from fittings of experimental data (Figs. 4, 5 and 6) $\Delta H_{\infty,calc}$, β and τ

	PMMA				PC			
	$\Delta H_{\infty,exp}$	$\Delta H_{\infty,calc}$	β	τ	$\Delta H_{\infty,exp}$	$\Delta H_{\infty,calc}$	β	τ
PC/PMMA-08	-	4.4 J/g	0.25	11400 s	-	3.8 J/g	0.23	14450 s
PC/PMMA-32	X	X	X	X	-	4.05 J/g	0.22	13350 s
PC/PMMA-1024	-	4.6 J/g	0.30	43650 s	1.45 J/g	2.24 J/g	0.31	130 s
PC/PMMA-4096	-	4.7 J/g	0.29	38050 s	0.94 J/g	1.32 J/g	0.46	34 s

(X: indicates that the values experimental are not available)

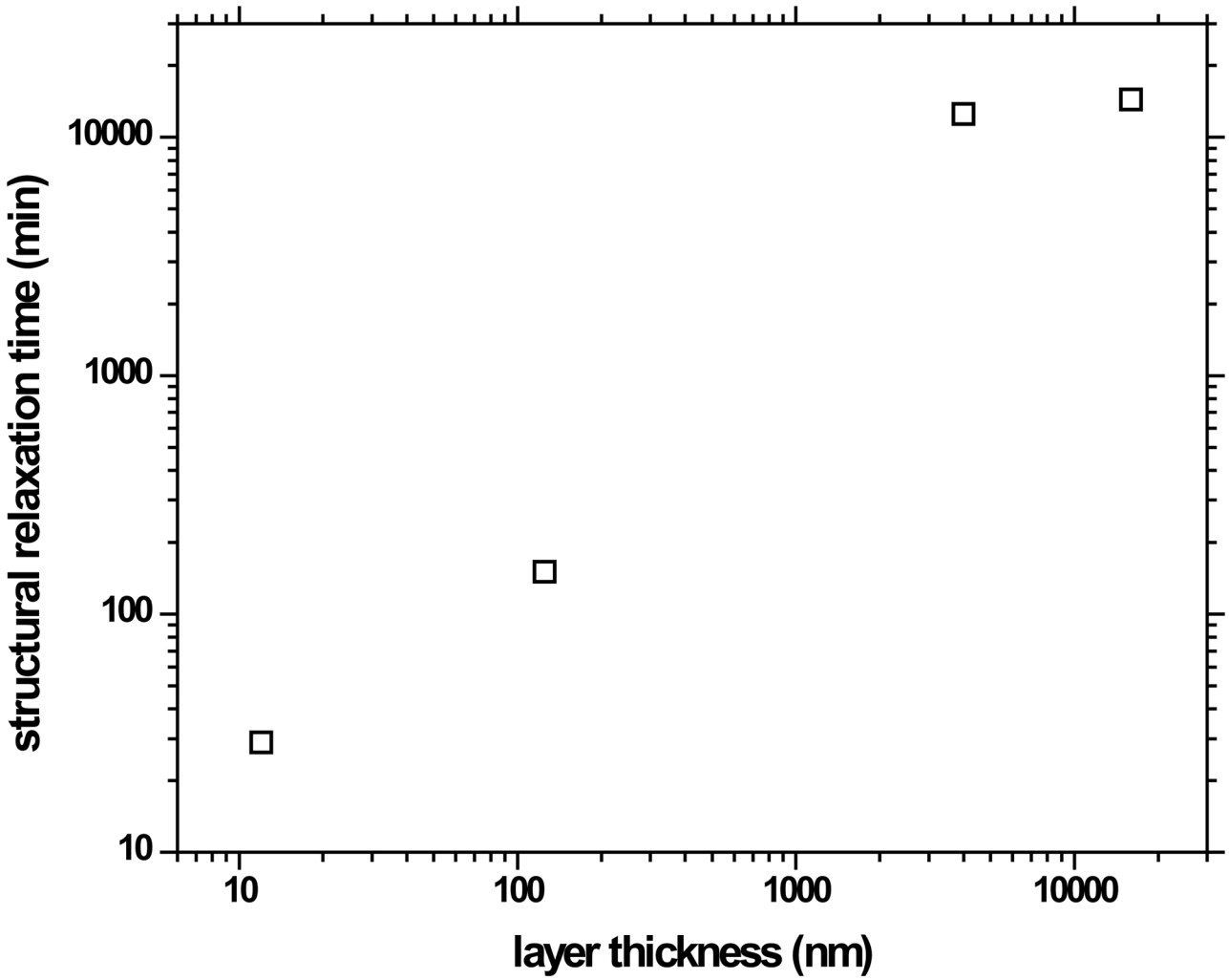

Fig. 7 Evolution of the structural relaxation time as a function of the aging time for PC obtained by the KWW model fitting

backbone) and no change in dynamic aging was observed. Consequently, the nature of the environment nano-scale can influence the aging. Note that this effect alone does not control the physical aging process.

The experimental results obtained on the accelerated aging of PC nanolayers which were attributed to the free volume interface caused by the state of the adjacent polymer (rubbery PMMA in this case) in nanolayered films and the absence of modification in PMMA nanolayers confirm the notion of change in the molecular mobility and the decrease or not of Tg in nano-scale films [57].

The physical aging acceleration may also be attributed to the polycarbonate molecular architecture (chain conformation) and to its influence on the relaxation processes occurring when this polymer is in confined environments. It is interesting to mention that the molecular mobility of PC is strongly influenced by the intramolecular and strong intermolecular interactions (Van der waalls, π stacking effects). These intermolecular interactions strongly influence cooperativity through glass transition. Therefore, the large network of intermolecular interactions in polycarbonate is an important factor for understanding the molecular mobility enhancement when the layer thickness is reduced to nanoscale.

The results of our study on the impact of the confinement of PMMA on its physical aging as well as its glass transition temperature (Tg) [57] agreed with those reported in the study carried out by Casalini and coworkers [84] who argued that the absence of a confinement effect on the cooperativity of PMMA layers confirms that the dynamic correlation length does not seem to be limited by the confinement geometry. This observation is related to the non-spherical cooperative regions. This asymmetry could be associated with the string-like shape seen in molecular dynamics simulations [85].

These results can be explained by the nature of movements responsible for α relaxation that seems to be related to

the shape of the CRR. For PMMA, the translation movement of the molecular chains (friction mechanism) is correlated with the relaxation (α); moreover, the local relaxation is mainly due to associated with the intramolecular interactions along the macromolecular chain. Consequently, one may state that the thickness reduction of the layers has very weak influence on the dynamics of the PMMA chains during aging.

Conclusion

The present work clearly shows that the confinement effect can have a significant impact on the physical aging process. The resulting changes may result in important industrial and scientific perspectives. A particular interest consists in understanding why some glasses are affected by the confinement effect while others are not, depending on their molecular structure and depending on the type of confinement they are submitted to.

Furthermore, aging of bulk and confined layered films (PC/PMMA), produced via layer-multiplying co-extrusion, was studied using differential scanning calorimetry (DSC).

In this study, the nature of molecular mobility (shape of CRR length linked to the intra-chain and inter-chain relaxation through glass transition), chemical structure and adjacent polymer state (rubbery and amorphous environment) appeared to have a huge impact on the physical aging process. Recovered enthalpy data for aged films showed an acceleration in physical aging with confinement for PC (the plateau is achieved in shorter time), while for PMMA, no change was observed. A reduction of the equilibrium enthalpy recovery, ΔH_∞, for PC layers submitted to a confinement effect has also been evidenced. These results are very consistent with those found in our previous work [57, 85] where the reduction in PC thickness was shown to have an impact on the glass transition parameters (Tα, ξ) and fragility index (m). Moreover, the correlation existing between fragility and cooperativity was attributed to the large modification of the activation volume around the macromolecules [86]. The decrease in the strong intermolecular interactions of the PC chains, as well as the resulting entanglement with the decrease in the thickness of layers and the soft-confinement effect due to rubbery layer at the interface of PC layers (PMMA layers) which acts as a free interface, all lead to disturbing the vitreous dynamics and accelerating the molecular mobility which impact directly the physical aging.

Acknowledgements E. Baer acknowledges the support of the NSF Center for Layered Polymeric Systems (Grant DMR-0423914). This work was carried out as part of the RMPP (Réseau Matériaux Polymères, Plasturgie) project. The authors acknowledge the financial support from "Région Haute-Normandie".

Data availability The data that support the findings of this study are available from the corresponding author upon reasonable request.

Declarations

Conflict of interest The authors declare no conflict of interest for this research paper.

References

1. Struik LGE (1978) Physical Aging in Amorphous Polymers and Other Materials. Elsevier Sci ltd, Amsterdam
2. Hutchinson JM (1995) Prog Polym Sci 20:703–4–760
3. Hall DB, Hooker JC, Orkelson JM (1997) Macromolecules 30:667–669
4. Alcoutlabi M, McKenna GB (2005) J Phys Condens Matter 17:R461
5. Keten S, Xu Z, Ihle B et al (2010) Nature Mater 9:359–367
6. Vogt BD (2017) J Polym Sci B: Pol Phys 56:9–30
7. Ko J, Kim Y, Kang JS, Berger R, Yoon H, Char K (2020) Adv Mater 32(10):1908087
8. Tagliazucchi M, Blaber MG, Schatz GC, Weiss EA, Szleifer I (2012) ACS Nano 6(9):8397–8406
9. Harton SE, Kumar SK, Yang H, Koga T, Hicks K, Lee H, Gidley DW (2010) Macromolecules 43(7):3415–3421
10. Roth CB (2021) Polymers under Nanoconfinement: Where Are We Now in Understanding Local Property Changes? Chem Soc Rev
11. Angell CA (1995) Formation of glasses from liquids and biopolymers. Science 267(5206):1924–1935
12. Novikov VN, Sokolov AP (2004) Nature 431(7011):961–963
13. Ko J, Berger R, Lee H, Yoon H, Cho J, Char K (2021) Chem Soc Rev 50(5):3585–3628
14. Demaggio GB, Frieze WE, Gidley DW, Zhu M, Hristov HA, Yee AF (1994) Phys Rev Lett 78:1524–1527
15. Jean YC, Zhang R, Cao H, Yuan J, Huang C, Nielsen B, Asoka-Kumar P (1997) Phys Rev B 56:R8459–R8462
16. Varnik F, Baschnagel J, Binder K (2002) Phys Rev E 65:021507–1–021507–14
17. Singh L, Ludovice PJ, Henderson CL (2004) Thin Solid Films 449:231–241
18. Seemann R, Jacobs K, Herminghaus S, Landfester K (2006) J Poly Sci: Part B: Polym Phys 44:2959–2968
19. Pye JE, Roth CB (2013) Macromolecules 46:9455–9463
20. Keddie JL, Jones RAL, Cory RA (1994) Europhy Lett 27:59–64
21. Bernazzani P, Sanchez RF, Woodward M, Williams S (2008) Thin Solid Films 516:7947–7951
22. Erber M, Khalyavina A, Eichhorn KJ, Voit BI (2010) Polymer 51:129–135
23. Erber M, Georgi U, Mûller J, Eichhorn KJ, Voit BI (2010) Eur Poly J 46:2240–2246
24. Parke K, Schneider RT, Siegel RW, Ozisik R, Cabanelas JC, Serrano B, Antonelli C, Baselga J (2010) Polymer 51:4891–4898
25. Xu G, Mattice WL (2003) J Chem Phys 118:5241–5244
26. Liu T, Siegel RW, Ozisik R (2010) Polymer 51:540–546
27. Yoshimoto K, Jain TS, Nealey PF, de Pablo JJ (2005) J Chem Phys 122:144712.1–144712. 6
28. Morita H, Tanaka K, Kajiyama T, Nishi T, Doi M (2006) Macromolecules 39:6233–6237
29. Amit S, Robert AR (2014) J Phys Chem B 118:9096–9103
30. Mittal J, Shah P, Truskett TM (2004) J Phys Chem B 108:19769–19779
31. Ngai KL (2003) Eur Phys J E 12:93–100

32. Oyerokun FT, Schweizer KS (2005) J Chem Phys 123: 224901.1–224901.13
33. Murphy TM, Langhe DS, Ponting M, Baer E, Freeman BD, Paul DR (2011) Polymer 5(2):6117–6125
34. Guo Y, Zhang C, Lai C, Priestley RD, D'Acunzi M, Fytas G (2011) ACS Nano 5:5365–5373
35. Cangialosia D, Alegríaa AC, Colmeneroa J (2016) Progre In Polym Sci 54:128–147
36. Murphy TM, Freeman BD, Paul DR (2013) Polymer 54:873–880
37. Cangialosi D, Boucher VM, Alegría A, Colmenero J (2012) Polymer 53:1362–1372
38. Boucher VM, Cangialosi D, Alegria A, Colmenero J, Pastoriza-Santosd I, Liz-Marzan LM (2011) Soft Matter 7:3607–3620
39. Tan AW, Torkelson JM (2016) Polymer 82:327–336
40. Mundra MK, Donthu S, Dravid V (2007) Torkelson. J Nano Letters 7:713–718
41. Roth CB, Dutcher JR (2005) J Elect Chem 584:13–22
42. Pfromm PH, Koroks WJ (1995) polymer 36: 2379–2387
43. Grohens Y, Hamon L, Reiter G, Soldera A, Holl Y (2002) Eur Phy J E 8:217–224
44. Priestley RD, Rittigstein P, Broadbelt LJ, Fukao K, Torkelson JM (2007) J phys Cond Matt 19: 205120.1–205120.12
45. Huang Y, Paul DR (2004) Polymer 49:3187–3204
46. Priestley RD, Ellison CJ, Broadbelt LJ, Torkelson JM (2005) Science 309:456–459
47. Priestley RD, Mundra MK, Barnett N, Torkelson JM (2007) Aust J Chem 60:765–771
48. Campbell CG, Vogt BD (2007) Polymer 48:7169–7175
49. Wübbenhorst M, Murray CA, Forrest JA, Dut JR (2002) Proceedings 11th International Symposium on Electrets 401:87–90
50. Wübbenhorst M, Lupascu V (2005) International Symposium on Electrets edition:12 location: Salvador 87
51. Schick C (2010) Eur Phys J Special Topics 189:3–36
52. Tran TA, Saïd S, Grohens Y (2005) Composites: Part A 36:461–465
53. Cangialosi D, Wubbenhorst M, Groenewold J, Mendes E, Schut H, van Veen A, Picken SJ (2004) Phys Rev B 70: 224213.1–224213.11
54. Gray LAG, Yoon SW, Pahner WA, Davidheiser JE, Roth CB (2012) Macromolecules 45:1701–1709
55. Langhe DS, Murphy TM, Shaver A, LaPorte C, Freeman BD, Paul DR, Baer E (2012) Polymer 53:1925–1931
56. Flores A, Arribas C, Fauth F, Khariwala D, Hiltner A, Baer E, Baltá-Calleja FJ, Ania F (2010) Polymer 51:4530–4539
57. Arabeche K, Delbreilh L, Adhikari R, Michler GH, Hiltner A, Baer E (2012) Polymer 53:1355–1361
58. Bernal-lara TE, Liu RYF, Hiltner A (2005) J Polymer 46:3043–3055
59. Delbreilh L, Bernès A, Lacabanne C, Grenet J, Saiter JM (2005) Mater Lett 59(23):2881–2885
60. Schammé B, Couvrat N, Malpeli P, Delbreilh L, Dupray V, Dargent É, Coquerel G (2015) Int J Pharm 490(1–2):248–257
61. McKenna GB, Jackson CL, O'Reilly JM, Sedita JS (1992) Poly Perprints 33:118–119
62. Rault J (2003) J Phys Condens Matter 15:S1193–S1213
63. Rabiei N, Amirshahi SH, Haghighat KM (2019) Phys Rev E 99(3):032502
64. Dobircau L, Delpouve N, Herbinet R, Domenek S, Le Pluart L, Delbreilh L, Ducruet V, Dargent E (2015) Polym Eng Sci 55(4):858–865
65. Delbreilh L, Negahban M, Benzohra M, Lacabanne C, Saiter JM (2009) J Therm Anal Calorim 96(3):865–871
66. Czerniecka-Kubicka A, Zarzyka I, Pyda M (2020) Molecules 25(17):3810
67. Puente JAS, Rijal B, Delbreilh L, Fatyeyeva K, Saiter A, Dargent E (2015) Polymer 76:213–219
68. Schammé B, Mignot M, Couvrat N, Tognetti V, Joubert L, Dupray V, Delbreilh L, Dargent E, Coquerel G (2016) J Phys Chem 120(30):7579–7592
69. Bourdet A, Esposito A, Thiyagarajan S, Delbreilh L, Affouard F, Knoop RJI, Dargent E (2018) Macromolecules 51(5):1937–1945
70. Tool AQ (1946) J Am Ceram Soc 29:240–253
71. Narayanaswamy OS (1971) J Am Ceram Soc 54:491–498
72. Moynihan CT, Ann NY (1976) Acad Sci 279:15
73. Mckenna GBJ (1994) Non-Cryst. Solids 172:756–764
74. Williams G, Watts DC (1970) Trans Faraday Soc 66:80–85
75. Vogel H (1921) Phys Z 22:645–646
76. Schonhals A, Goring H, Schick C (2002) J Non Cryst Solids 305:140–149
77. Roth CB (2021) Chem Soc Rev
78. Priestley RD (2009) Soft Matter 5(5):919–926
79. Cangialosi D, (2018) Chapter 8 - Glass Transition and Physical Aging of Confined Polymers Investigated by Calorimetric Techniques. In Handbook of Thermal Analysis and Calorimetry, Elsevier Science B V 6:301–337
80. Monnier X, Fernandes Nassar S, Domenek S, Guinault A, Sollogoub C, Dargent E, Delpouve N (2018) Polymer 150:1–9
81. Morvan A, Delpouve N, Vella A, Saiter-Fourcin A (2021) J Non-Cryst Solids 570:121013
82. Roth CB, Torkelson JM (2007) Macromolecules 40:3328–3336
83. Lewis EA, Vogt BD (2018) J Polym Sci Part B: Polym Phys 56:53–61
84. Casalini R, Zhub L, Baerb E, Rolanda CM (2016) Polymer 88:133–136
85. Hanakata PZ, Douglas JF, Starr FW (2014) Nat Commun 5:4163–4170
86. Arabeche K, Delbreilh L, Saiter JM, Michler GH, Adhikari R, Baer E (2014) Polymer 55:1546–1551